INSTITUTE OF PHYSICS PUBLISHING JOURNAL OF PHYSICS B: ATOMIC, MOLECULAR AND OPTICAL PHYSICS

J. Phys. B: At. Mol. Opt. Phys. **36** (2003) 4875–4888 PII: S0953-4075(03)69599-4

Coplanar symmetric (e, 2e) measurements from calcium at low energy

Andrew James Murray and Danica Cvejanovic

Schuster Laboratory, The University of Manchester, Manchester M13 9PL, UK

E-mail: Andrew.Murray@man.ac.uk

Received 25 September 2003
Published 21 November 2003
Online at stacks.iop.org/JPhysB/36/4875

Abstract

Coplanar symmetric (e, 2e) results are presented for the ionization of calcium by electron impact. The incident electron energy was varied from 10.1 to 64.6 eV, the outgoing electrons sharing the excess energy equally. The experimental results show a complex variation in the magnitude of the cross-section as a function of energy and angle. At the highest incident energy, the cross-section varies by almost five orders of magnitude. At the lowest energy, evidence of post-collisional interaction between the outgoing electrons can be seen, although the magnitude of this effect is small.

S This article has associated online supplementary data files

(Some figures in this article are in colour only in the electronic version)

1. Introduction

The study of electron impact ionization of atoms and molecules has been of interest since the early days of atomic and molecular physics, since the energetics of this process are easily controlled, and the electrons or ions resulting from the reaction can be observed with relative ease. Experimental techniques for controlling the momentum of the incident electron beam are well established, as are methods to determine accurately the momenta of the scattered and ejected electrons (or ions) that result from the reaction [1–3].

The most complex interaction occurs when an electron ionizes the target. In this case there is one charged particle in the incident channel, and three (or more) charged particles in the final channel. As the incident electron approaches, the neutral target will be polarized by the incoming electron, and the interaction produces distortions in the incoming wave. Multiple scattering may occur during the interaction, resulting in the incident and ejected electrons being scattered over a wide range of angles. After ionization the electrons interact dynamically with each other and with the residual ionic core in a complex many-body reaction which continues over a long range. This interaction will lead to momentum being exchanged between the

outgoing particles, and so they may emerge with a very different trajectory to that which they had immediately following the reaction [4, 5].

The complexity of the ionization process means that experiments are often difficult, and theoretical models that describe the interaction must of necessity include approximations to make the calculations tractable. A number of different theories have been developed, ranging from first-order Born calculations (and variations therein) which are successful at high incident energies and asymmetric geometries [6] to second- and higher order Born calculations which are successful at higher energies in more complex scattering geometries [7]. Variants on these models include distorted wave Born approximations (DWBAs) that have achieved success down to intermediate energies [8–11]. These models introduce distortions into the wavefunctions representing the electron trajectories, and so more closely approximate the interaction. DWBA models now also include post-collisional interactions in the final channel [12]. This has improved the comparison between theory and experiment, and has allowed the model to reach to lower energies. At very low energies the Wannier model and its quantum mechanical derivatives have proven to be successful [13–15]. In this approximation, post-collisional interactions dominate and strongly influence the final electron yield.

Other models have also been developed to describe the reaction. The close coupled channel (CCC) theory and its derivatives have proven to be very successful at modelling excitation by electron impact [16], and these theories are being refined to study ionization. Since the CCC theory uses a basis set of pseudo-states that reaches into the continuum, this theory should also be able to model ionization from threshold through to higher energies, providing sufficient accurate basis states are employed.

Experimentally, the most detailed information that can be obtained about the ionization process requires the products of the reaction to be measured in coincidence. For single ionization, it is only necessary to determine the momenta of the scattered and ejected electrons, since the momentum of the ion can then be inferred. The scattering process is known as an (e, 2e) reaction, and it is necessary to measure the angular correlation that occurs between the scattered and ejected electrons to allow comparison with theory.

A wide range of momenta of the outgoing electrons are possible within the constraints that energy and momentum must be conserved. In the reference frame of the target:

$$\begin{aligned} E_{\mathrm{inc}} &= E_{\mathrm{a}} + E_{\mathrm{b}} + \mathrm{IP} \\ \mathbf{k}_0 &= \mathbf{k}_{\mathrm{a}} + \mathbf{k}_{\mathrm{b}} + \mathbf{k}_{\mathrm{ion}} \end{aligned} \tag{1}$$

where E_{inc} is the energy of the incident electron of momentum $\mathbf{k}_0$, IP is the energy required to ionize the target, E_{a}, E_{b} are the energies of the outgoing electrons with momenta $\mathbf{k}_{\mathrm{a}}$, $\mathbf{k}_{\mathrm{b}}$ and $\mathbf{k}_{\mathrm{ion}}$ is the recoil momentum of the ion following the reaction. These equations place no constraints on the relative momenta of the outgoing electrons and so it is possible to measure correlated electrons over a wide range of geometries and energies.

The complexity of the interaction means that experiments usually only measure a subset of the reaction channels that are possible. The most usual geometry that is chosen is coplanar geometry, where $\mathbf{k}_0$, $\mathbf{k}_{\mathrm{a}}$ and $\mathbf{k}_{\mathrm{b}}$ all lie in the same plane, although measurements in other geometries have also been conducted [4, 17–21]. A coplanar symmetric geometry is adopted in the experiments described here, where the correlated electrons are further constrained so that $|\mathbf{k}_{\mathrm{a}}| = |\mathbf{k}_{\mathrm{b}}|$ and the electrons are measured at equal angles $\xi_{\mathrm{a}} = \xi_{\mathrm{b}} = \xi$ with respect to the incident electron direction.

Comparison between theory and experiment is made through the triple differential cross-section, which is defined as a function of the outgoing electron energy and the direction of the scattered and ejected electrons. In the coplanar symmetric case, the cross-section only depends on the mutual angle ξ and the energy:

$$\frac{\mathrm{d}^3\sigma}{\mathrm{d}E_\mathrm{a}\,\mathrm{d}\Omega_\mathrm{a}\,\mathrm{d}\Omega_\mathrm{b}} = \frac{\mathrm{d}^3\sigma}{\mathrm{d}E_\mathrm{a}\,\mathrm{d}\Omega_\mathrm{a}\,\mathrm{d}\Omega_\mathrm{b}}(E_\mathrm{a}, \xi). \tag{2}$$

In the experiment the incident electron energy E_inc is set, and electrons of equal energy $E_\mathrm{a} = E_\mathrm{b} = (E_\mathrm{inc} - \mathrm{IP})/2$ are detected in coincidence at equal angles $\xi_\mathrm{a} = \xi_\mathrm{b} = \xi$. The analysers then move to a different angle, and the experiment is repeated until a complete set of data is obtained. By configuring the experiment to have constant electron beam current and target density throughout these measurements, the results can be normalized to produce the differential cross-section as defined in equation (2). It is more difficult to compare results at different energies, since experimental parameters such as the focusing of the electron gun and analysers changes with energy. These have not been considered in the experiments described here, and so the relative magnitudes cannot be compared as a function of the incident energy.

The target which has been used in these studies is calcium, which is an alkali earth atom with a ground state configuration $(4s^2)^1S_0$. Calcium has a similar structure to the $(1s^2)^1S_0$ ground state of helium, and so might be expected to show similarities in the measured cross-sections. The inner electrons may also play a significant role in the ionization reaction, and so must also be considered. The proximity of the closely lying empty 3d orbital to the 4s shell in calcium has been found to influence the photo-ionization process significantly at low energy [29], and so this may also influence the (e, 2e) reactions studied here.

There have been a number of photo-ionization studies carried out on calcium, which detail resonances in the ionization cross-section [22–29]. By contrast, there are far fewer electron impact ionization experiments. Early studies measured total ionization cross-sections by detecting the ions as a function of the incident electron energy [30–34]. Recent experiments by Cvejanovic and Murray [35] also measured the ion yield as a function of impact energy, and placed the results on an absolute scale by normalizing to the ionization cross-section for H_2O which is well known. These new results showed similarities to the early cross-section measurements, but clear differences were seen in both the magnitude and structure.

Electron impact ionization experiments reported so far include those at high energy which studied ionization in the 2p and 3p auto-ionizing regions [36–40]. Kleinpoppen and co-workers [41] studied the simultaneous ionization and excitation of calcium by measuring fluorescence from the $4\,^2P_{3/2}$–$4\,^2S_{1/2}$ line in the residual ion, whereas Crowe and co-workers are currently setting up experiments to measure triple coincidences from electron-induced ionization and excitation of the ion [42].

No (e, 2e) studies of calcium have so far been reported. There have been extensive studies of other metal targets, including sodium which has been ionized from the ground state [43] and from the laser-prepared ^2P state [44–46]. Other alkali targets that have been investigated are potassium [47], lithium [48] and rubidium [49]. Magnesium is the only alkali earth to have been studied so far, and these measurements were conducted in a coplanar asymmetric geometry [50]. Martin and co-workers have extensively studied the ionization of cadmium in both the direct and auto-ionizing regions of the ionization spectrum [51–55], and measurements have also been reported for very high-energy (e, 2e) studies from gold [56, 57].

Experiments involving metal vapours are considerably more challenging than those using gaseous targets, since it is necessary to produce a beam of atoms in the gas phase by heating in an oven, often at high temperatures. Several complications can arise which are not normally considered for gaseous targets. The heat of the oven can cause expansion inside the spectrometer, which may result in loss of alignment. If the metal vapour re-condenses onto surfaces inside the spectrometer, this can significantly alter the properties of the apparatus. As an example, the contact potentials around the interaction region may vary as deposition occurs, and this must be considered when analysing the data. A more serious problem occurs when the

vapour deposits onto the electron optics inside the electron gun (and to a lesser extent inside the analysers) since this leads to charging of the surfaces by stray electrons, with a subsequent degradation of beam quality.

To minimize these effects, the oven is operated in a temperature regime where the atomic beam is spatially well defined. The target density in the interaction region is therefore smaller than can be produced using gaseous targets, with a subsequent reduction of coincidence yield. The experiments therefore must operate for longer accumulation times, which can further aggravate instabilities in the system. Careful design of the spectrometer, together with methods to collect the metal vapour efficiently, are therefore essential, and techniques that have been adopted in the spectrometer at Manchester are detailed here.

This paper is divide into five sections. In section 2 the (e, 2e) apparatus is described. The spectrometer has been detailed in a number of publications [17–21, 58]; however, substantial changes have been made for the new experiments reported here. Problems associated with calcium are discussed in this section, together with the techniques used to solve these. Elastic, inelastic and superelastic scattering processes were all used to investigate and solve problems to ensure a reliable coincidence signal was obtained, and these studies are mentioned in this section. The experimental results are presented in section 3, taken from a low incident energy of 10.1 eV through to the intermediate-energy regime at 64.6 eV. The (e, 2e) results are discussed in section 4, and comparisons are made with measurements ionizing helium. Section 5 draws conclusions from these data.

2. The experimental apparatus

Figure 1 shows the apparatus which is used in these studies. A number of changes have been made so that experiments on calcium can be conducted. These changes evolved over time as the difficulties associated with working with calcium were addressed. Since the spectrometer operates over a wide range of different geometries, installation of new components needed to ensure that the angles through which the gun and analysers could move were not compromised. This led to restrictions on the design of these components, and their location inside the spectrometer.

One of the main changes to the spectrometer was the installation of the atomic beam oven, which was designed to occupy the same position as a photomultiplier tube (PMT) used in previous studies [58]. The oven was mounted onto the electron gun yoke as shown in figure 1, and so moved with the electron gun when rotated from $\psi = 90^\circ$ (the perpendicular plane as shown) to $\psi = 0^\circ$ (the coplanar geometry). The oven mounting system allowed the oven to be accurately directed to the interaction region, so that the output nozzle was positioned $\sim$6 mm from the interaction region.

The original oven designed for these experiments used a two-stage heater surrounding the calcium crucible [59]. The crucible was constructed in two parts, a lower chamber which contained the calcium and an upper chamber which directed the beam to the target via a hypodermic needle. The two chambers were connected via a CF34 flange, the seal being made using a copper gasket. This design operated reliably at first, but after time the oven breached at the flange, and calcium effused into the vacuum chamber. Upon inspection it was noted that the calcium vapour had strongly reacted with the copper gasket until it was no longer serviceable.

To solve this problem, the oven was reassembled without a gasket, and was again found to operate for only a short time before a marked reduction in beam density was observed. This reduction was due to the crucible being ‘choked’ internally by solid calcium depositing at the flange interface between the lower and upper chambers. This problem arose since the flange was not directly heated, and so was slightly cooler than the lower and upper chambers.

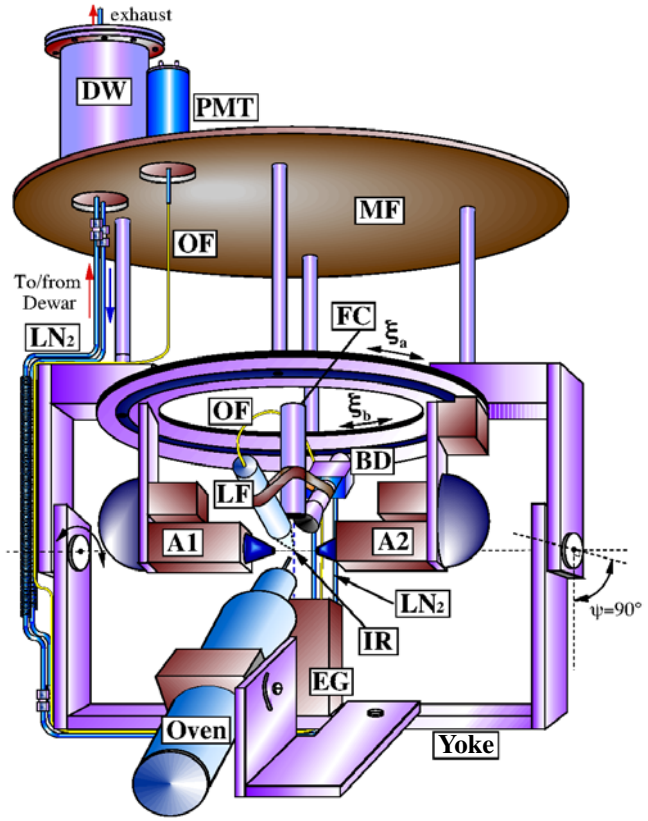

Figure 1. The (e, 2e) spectrometer at Manchester which has been reconfigured for experiments ionizing calcium. The analysers A1 and A2 rotate in the horizontal detection plane, whereas the electron gun (EG) can rotate from $\psi = 90°$ (the perpendicular plane geometry) to $\psi = 0°$ (coplanar geometry). The Faraday cup (FC), atomic beam oven, beam dump (BD) and lens/fibre (LF) assembly all rotate with the EG. The BD is cooled by liquid nitrogen gravity fed from the Dewar (DW) through stainless steel tubes and flexible pipes (LN_2). Light from the interaction region is focused by the lens into a 400 μm optical fibre (OF) which carries the light to a photomultiplier tube (PMT) located on the main flange (MF).

Calcium sublimes directly from the solid to the gas phase, and so had condensed onto the cooler flange, rapidly accumulating to become a solid mass between the chambers.

Although a number of different techniques were attempted to alleviate this problem, it reoccurred each time the oven operated, and so a new crucible was designed. The new crucible is made from a single block of 310-grade stainless steel, the entrance to the oven being through a plug in the base of the lower section (see figure 2). This design used the same heaters as for the old oven, and was found to eliminate the choking problems with the original design. An additional copper jacket thermally connected to the upper and lower heaters was placed around the new crucible to ensure that all parts were heated.

The oven crucible and heater assembly was surrounded by four stainless steel shields to reduce thermal emission into the vacuum chamber. The lower chamber was operated at a temperature of 600 °C and the upper chamber was held at 630 °C. The heat shields served the dual purpose of reducing the power required to heat the oven while minimizing heat loss. The temperature of the surrounding regions was monitored using copper–constantan thermocouples, and the electron gun and oven mount were found to reach temperatures of

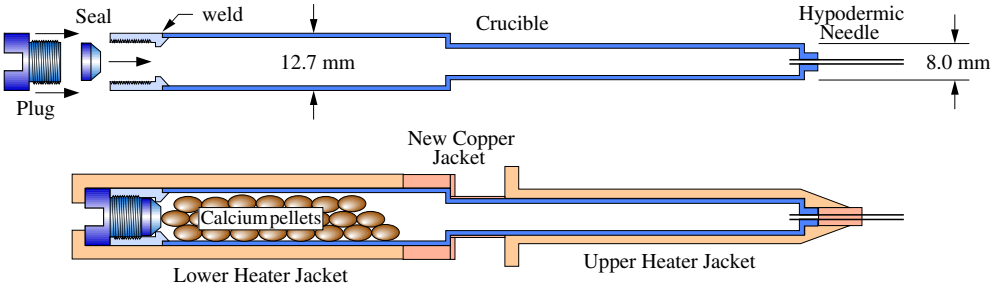

Figure 2. The new oven crucible, drawn to scale. The seal is accomplished using a stainless steel plug/seal assembly through the base of the crucible after loading calcium pellets into the oven under argon. The crucible is heated by a lower and upper heater jacket, a new middle copper jacket connecting to the upper and lower heaters providing good thermal contact over the complete surface of the crucible.

80 °C with the oven operating for several days. No significant effects due to heating were seen in either the gun or oven; however, the internal gear assembly to analyser 1 seized due to thermal expansion. This was alleviated by using a flexible coupling inside the vacuum chamber to allow for expansion of the drive assembly.

The second major change to the spectrometer was the installation of a liquid-nitrogen-cooled beam dump (BD) located directly opposite the output nozzle of the oven. It was essential that most of the calcium emission was contained, or the electron optics became very unstable. A water-cooled beam dump was initially tried but this proved to be inadequate, and so a liquid nitrogen dewar (DW) was designed and installed onto the main flange (MF) of the spectrometer [60]. To ensure the beam dump was at liquid nitrogen temperatures, the nitrogen was gravity fed from the dewar through flexible stainless steel tubing to a small 310-grade stainless steel chamber enclosing the beam dump. The tubing was insulated from and secured to the electron gun yoke to allow the electron gun, oven, Faraday cup (FC) and beam dump to all rotate around the gun axis.

During operation the dewar was filled with 5 litres of liquid nitrogen. At the initial fill it was essential to ensure that there were no vapour locks in the internal feed tubing, and this was achieved by pumping on the exhaust line with a small rotary pump. After filling the dewar the temperature of the beam dump rapidly reduced until a temperature of −185 °C was reached. At this time the chamber surrounding the beam dump was full of liquid nitrogen, and the amount of nitrogen gas which was boiling off reduced. Since the beam dump, feeder tubing and dewar were full of liquid nitrogen, their surfaces acted as a pump for water vapour inside the chamber, and the background pressure reduced to $\sim 1.5 \times 10^{-8}$ Torr.

With the oven operating at normal temperature, the liquid nitrogen boil-off rate increased, but the heat shielding around the oven minimized this loss. The dewar charge was designed to last 12 h when the oven was cold. This reduced to 6 h with the oven operating, and so an automatic filler was built to maintain liquid in the dewar while the experiment was being conducted [61].

The (e, 2e) spectrometer at Manchester is a fully computer-controlled system that is also computer optimized. Part of the optimization routine steers and focuses the electron beam onto the interaction region by observing fluorescence arising from excitation of the target by the electron beam. To monitor this fluorescence, a lens (LF) of 25 mm focal length and 12 mm diameter focused light from the interaction region onto the core of a 400 μm optical fibre (OF) which was directed to a photomultiplier tube (PMT) located externally on the top flange. The lens and fibre assembly was connected to the Faraday cup, so that this also rotated with the electron gun.

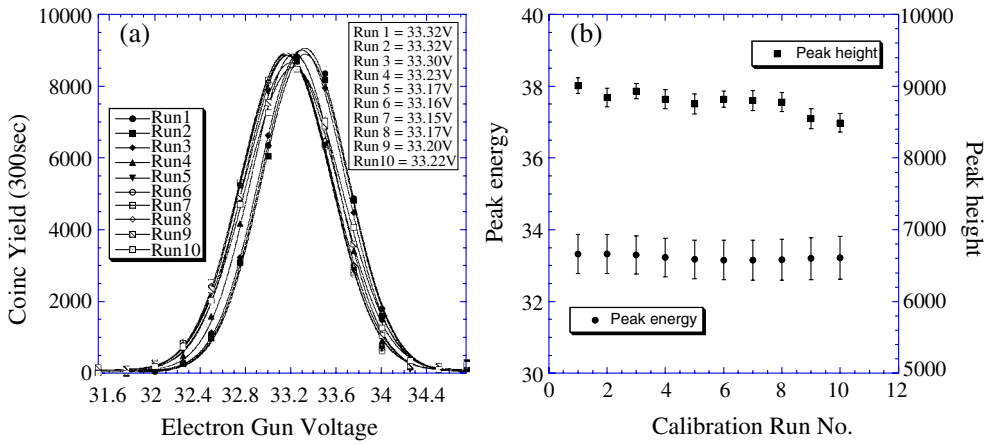

Figure 3. Coincidence energy spectra from calcium at a nominal energy of 34.6 eV. The spectra are fitted with Gaussian profiles to determine the peak position, width and intensity of the coincidence signal in (a). The variations in peak height and position are shown in (b), the data having been taken over an 11 h period.

A major problem with this arrangement was found to be due to calcium depositing onto the lens. After 3 days, the photon count rate had reduced to 50% of that first observed. The changing photon yield therefore could not be used to normalize the coincidence signal over time, as was done for gaseous targets. The photon count rate could be used to optimize the electron gun at the start of the experiment, but this became impossible as the rate declined with time. After 2 weeks of operation the vacuum chamber had to be opened to remove calcium deposition from the lens and other sensitive parts of the spectrometer.

It was also important to ascertain the effects of calcium deposition on the electron optics inside the spectrometer. The energy of the incident and detected electrons was observed to change due to this deposition, and several different methods were used to quantify these effects. To establish the effect on the incident electron energy, helium was input to the chamber and the $2\,^2S$ resonance in the elastic scattering signal at 19.336 eV [62] was measured as a function of the gun voltage. This resonance depends only on the incident energy, and so changes to the contact potential could be determined as the oven heated and calcium deposited onto surfaces. The contact potential was found to vary by around 1 eV as deposition occurred, but after a few days this stabilized to a constant value.

The effects of calcium deposition on the analysers was determined by observing the inelastic scattering of electrons from helium, argon and calcium while the oven was operating. The analysers were adjusted so that the energy loss spectra matched the incident electron beam energy. Changes were initially observed, but these again stabilized over time.

Finally, the effect of calcium deposition on the correlated signal was determined over time by monitoring the (e, 2e) signal as a function of the incident electron energy. As an example, a series of coincidence energy spectra is shown in figure 3(a), taken over a time period of 11 h following stabilization. The analysers were set to a pass energy of 14.25 eV at a scattering angle $\xi_a = \xi_b = 35°$ for these experiments. The incident electron energy ranged from 31.5 to 34.75 eV in 250 meV intervals, and the coincidence signal was accumulated for 300 s at each energy.

Figure 3(b) shows the results of these measurements. The peak height is seen slowly to decrease to 95% of the initial value, indicating that the atomic beam density was slightly

changing. The variation in peak position is also shown in this figure, the error bars being taken from the width of the fitted Gaussian curves. The peak is seen to drift ∼150 meV over this time period. The expected energy for the peak was 34.6 eV, and the difference of −1.3 eV seen here is predominantly due to calcium deposition.

Once the system had stabilized in energy, the electron gun was set to the peak position determined from a coincidence energy curve as in figure 3(a). To ensure that the spectrometer remained optimized throughout data accumulation, an energy spectrum was accumulated after each sweep of the detection plane by the analysers. Corrections were then made to the incident energy to allow for small changes in the peak energy.

It is clear from the above discussions that the major problem in the experiment is due to calcium deposition onto surfaces near the interaction region. Improvements are currently under way to improve the directivity of the atomic beam (thereby reducing the amount of calcium deposited directly from the source) and to enhance trapping by the beam dump. Once these modifications are made, it is expected that the spectrometer will be considerably more stable, and will not need to be cleaned as frequently.

3. Experimental results

The main aim of the current (e, 2e) research programme at Manchester is to measure signals from *laser-excited* calcium, as this allows the ionization process to be determined in greater detail than from a target in the ground state. Additional information is obtained in this process since the laser-excited target can be oriented and aligned with respect to the interaction geometry, thereby reducing the symmetry of the scattering process. The sensitivity of the interaction to the laser-prepared target structure can then be determined over a complete range of scattering geometries [63].

The experiments described in this paper were carried out as part of the development of these laser-based experiments. It was necessary to measure the yield directly prior to attempting the more difficult experiments, and so two different experiments were conducted. The first measured the direct ionization of calcium in coplanar geometry, and it is these experiments that are detailed here. The second studied the effects of laser preparation of the target by measuring the superelastic scattering yield as a function of the scattering geometry. The results from these experiments have recently been submitted for publication [64].

Initial (e, 2e) measurements from laser-excited calcium have also now been carried out. In these experiments the cross-section was measured as a function of the laser polarization direction in coplanar geometry at an angle $\xi = 35^\circ$ for an incident energy of 34.6 eV [65]. Unfortunately these very recent experiments have been halted at present due to lack of funding.

The direct (e, 2e) measurements reported here were carried out with an incident electron energy ranging from 10.1 to 64.6 eV to determine the cross-section over as wide a range of energies as possible. The incident energy could not be reduced below 10.1 eV due to difficulties focusing the incident beam onto the target, whereas the higher energy limit was due to difficulties focusing the analysers onto the interaction region.

Figure 4 shows the coplanar symmetric results, all plotted on the same relative scale. Eight different energies were selected: $E_{\mathrm{inc}} = 10.1$, 12.1, 19.6, 24.6, 34.6, 44.6, 54.6 and 64.6 eV. These energies were chosen to allow comparison with results from helium at similar energies. No absolute measurements were made, and so the magnitudes of the cross-sections were renormalized to unity for a scattering angle $\xi = 45^\circ$ at each energy.

The incident electron beam current used for these studies ranged from 200 nA at 10.1 eV to 2.5 μA at 34.6 eV and above. The results were collected over a period of 10 months, with frequent intervention required in the early stages to clean the apparatus when the system

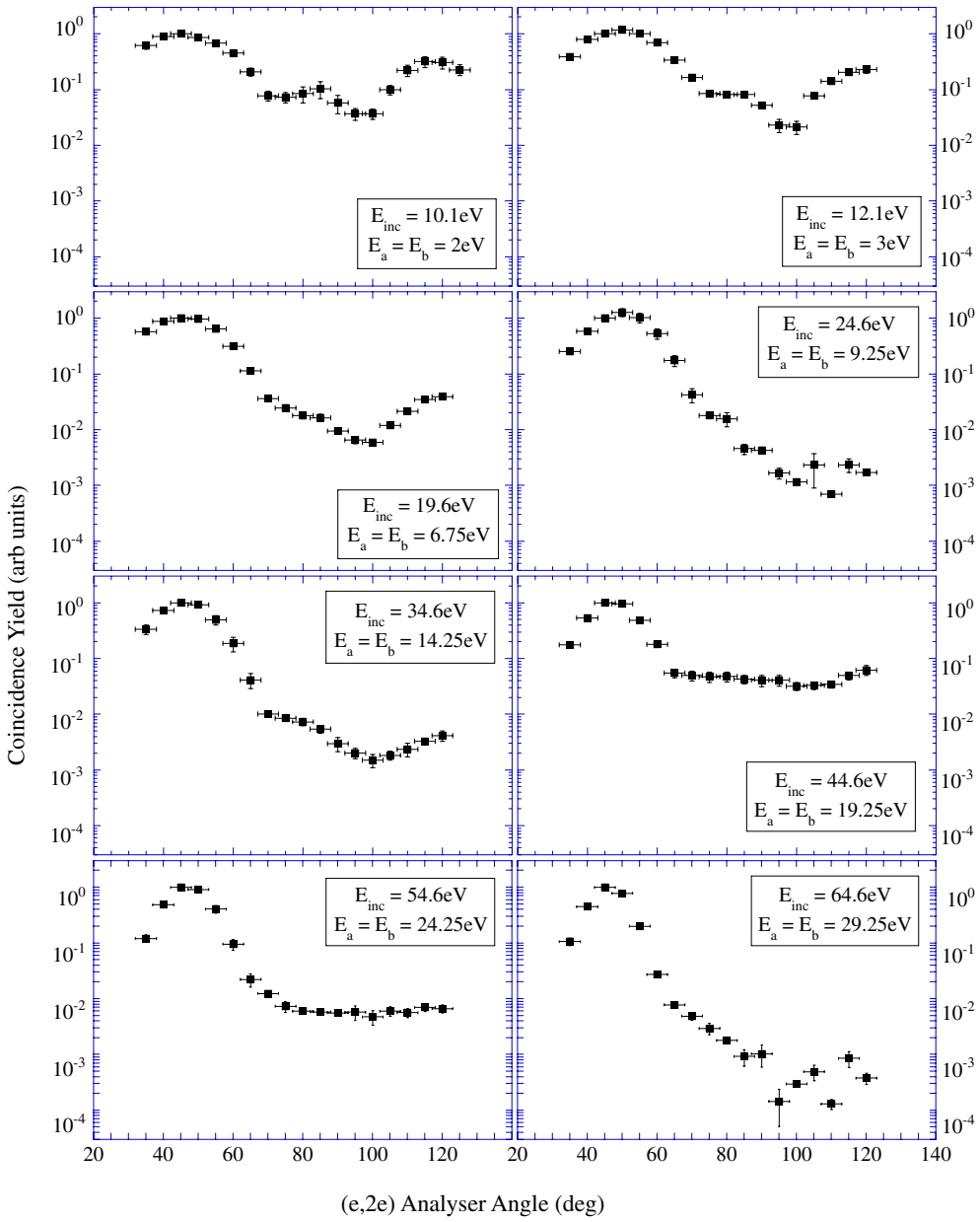

Figure 4. Differential cross-sections for the ionization of calcium over a range of incident energies in a coplanar symmetric geometry. The data are all normalized to unity at a scattering angle $\xi = 45°$. The analysers are constrained between $\xi = 35°$ and 120° by the electron gun and Faraday cup. At scattering angles $\xi = 0°$ and 180° the cross-section must reduce to zero due to post-collisional interaction between the outgoing electrons. For details, see text.

M Supplementary data files are available from stacks.iop.org/JPhysB/36/4875

became unstable. The data were collected using the computer control systems which were set to move and optimize the analysers, but the routine to tune the gun was defeated as it was

difficult to optimize to photon counts as discussed above. A coincidence energy spectrum was taken after each sweep of the scattering plane to correct for any energy drifts due to calcium deposition. The data at each energy were then averaged, and the error bars in the results reflect the variation around this average.

The typical operating conditions throughout data collection were as follows. The oven temperature was set to 600 °C for the body and 630 °C for the nozzle by passing a current of 0.65 A through the body heater and 0.7 A through the nozzle heater. The heaters were supplied by custom-built constant current supplies which maintained the temperatures of the body and nozzle at a constant value with a variation of only $\pm 3°$. It is very difficult to estimate the beam density from the oven as it depends on many factors, and so the temperature was selected to produce good coincidence yield while minimizing the effects of calcium deposition. The base pressure inside the chamber was $\sim 1.5 \times 10^{-8}$ Torr and this was seen to rise to $\sim 4 \times 10^{-8}$ Torr under operating conditions. This working pressure does not accurately reflect the true beam density as most of the calcium inside the spectrometer would condense onto surfaces prior to reaching the ionization gauge.

The electron beam current measured by the Faraday cup was monitored throughout the experimental runs by the computer control systems, and deviations were considered in the data analysis. The current was adjusted to minimize the effects of surface charging by the beam, which could not be focused well at lower energies. It was very difficult to produce consistent results at energies below 15 eV due to these instabilities, and this is reflected in the larger variations seen in the data.

Typical count rates varied greatly, depending on the conditions of the experiment. The analyser count rates were kept below 50 kHz to reduce the effects of pileup in the coincidence counting electronics, which had been observed in previous studies with this apparatus. The coincidence count rate varied between 100 s^{-1} and <1 h^{-1}, depending on the energy and scattering angle. To improve the statistics at low rates of accumulation, data were collected for significantly longer times compared with that used for the higher rates.

The data presented in figure 4 show a large variation in the relative cross-section as a function of energy. All data are presented on a logarithmic scale, and it is clear that the cross-section does not vary monotonically with energy. The angular shape of the cross-section evolves reasonably smoothly with energy, although variations in this structure are observed. A dominant peak can be seen in the forward direction at $\xi \sim 50°$ for all energies. The data show a second peak in the backward direction at $\xi \sim 120°$ for lower energies which disappears at 24.6 eV, only to reappear at 34.6 and 44.6 eV before once more becoming small at higher energies. The ratio of backward peak intensity to the forward peak is largest at the lowest incident energy.

A structure at $\xi \sim 80°$ for energies from 10.1 to 34.6 eV disappears at 44.6 eV and higher energies, where the cross-section flattens off. The increase in the relative cross-section between 24.6 and 44.6 eV warrants further exploration over a finer energy mesh to determine how this structure evolves. At 44.6 eV the cross-section flattens off at scattering angles $\xi > 60°$, and this flatness continues to 54.6 eV with an overall decrease in relative magnitude. At 64.6 eV the higher angle results are difficult to interpret due to the very low count rates, but the flat structure appears to have diminished, and there is little evidence of a backscatter peak. At this energy the cross-section varies by almost five orders of magnitude over the range of angles that have been explored. It should be noted that the cross-section must be zero at $\xi = 0°$ and 180° for all measurements due to post-collisional interactions between the outgoing electrons.

The complete set of data can be downloaded as a text file for further analysis by linking to the electronic version of this paper.

4. Comparison to helium

Prior to these experiments the cross-sections from calcium were expected to be similar to helium, since both targets have the same valence shell structure. By contrast, the actual results are very different. This comparison can be made in a number of different ways. To describe the effects of post-collisional interactions, the energy of the outgoing electrons plays an important role, whereas the energy of the incident, scattered and ejected electrons is important in detailing the collision dynamics. The ionization potential of helium is 24.6 eV, whereas the ionization potential of calcium is 6.11 eV and so the energy scale of the electrons relative to the ionization potential is quite different for the two targets.

To allow comparison between these targets, experimental results for helium in a coplanar geometry are plotted on a logarithmic scale in figure 5, again normalized to unity at $\xi = 45°$. The results at the lowest energy are from Selles and co-workers [66], while the remaining data were collected using the (e, 2e) spectrometer at Manchester [67, 68]. The incident energy ranged from 26.6 to 74.6 eV, and so spans a similar range as for calcium. Further, the outgoing electron energies varied from 2 to 50 eV above the helium threshold, and so the effects of post-collisional interactions following collision at low energy can be considered.

The contrast between the results for helium and calcium is striking. At the lowest energies corresponding to outgoing energies up to 1.5 eV, the helium results agree well with the Wannier model which describes the cross-section by a modified single Gaussian peaking at $\xi = 90°$ [68]. Even at an outgoing energy of 2.5 eV ($E_{\mathrm{inc}} = 29.6$ eV), the helium results show a single structure which evolves into two peaks at higher energies. The single peak at lower energies is due to post-collisional interactions dominating the cross-section. In this energy region the outgoing electrons strongly interact to repel each other, resulting in a maximum yield at a mutual angle $\xi_{\mathrm{a}} + \xi_{\mathrm{b}} = 180°$ as is observed.

By contrast, the low-energy results for calcium show a three-peak structure, with the forward peak dominating. It is likely that at these energies the central peak at $\xi \sim 80°$ has a contribution due to post-collisional interactions, but since this peak is visible for outgoing electron energies up to 14.25 eV, other factors must be contributing. At the lowest outgoing energy ($E_{\mathrm{a}} = E_{\mathrm{b}} = 2$ eV), the forward and backward peaks dominate, the ratio of peak heights to the central peak being 8:1 and 4:1 respectively. The forward peak is usually considered to be due to a simple binary collision between the incoming electron and valence electron, whereas the backscatter peak is considered to be due to elastic scattering of the incident electron from the target, followed by a binary collision into the backward direction. Both of these processes seem to be occurring in calcium with much greater probability than for helium, and the simple Wannier model does not apply. It is likely that other electrons in the calcium ion core are also playing a significant role in the interaction, and so the dynamics of these electron correlations will need to be carefully considered.

At incident electron energies above 34.6 eV, the results for helium show a smooth variation with energy, the backscatter peak steadily reducing compared with the forward scattering peak. The peaks have equal magnitude around 50 eV, and the dip in the cross-section at $\xi \sim 70°$ becomes more pronounced. These measurements have been predicted with reasonable success using DWBA models [69]. By contrast, the higher energy results for calcium show complex variation in magnitude as a function of incident energy and scattering angle as has been described above. It is likely that this is again due to electron correlations between the measured electrons and those remaining in the core, an effect that does not contribute as significantly for helium.

5. Conclusions

The data presented here are the first coplanar symmetric low-energy (e, 2e) measurements from an alkali earth target. The results indicate that the simple idea that the ionization process mainly

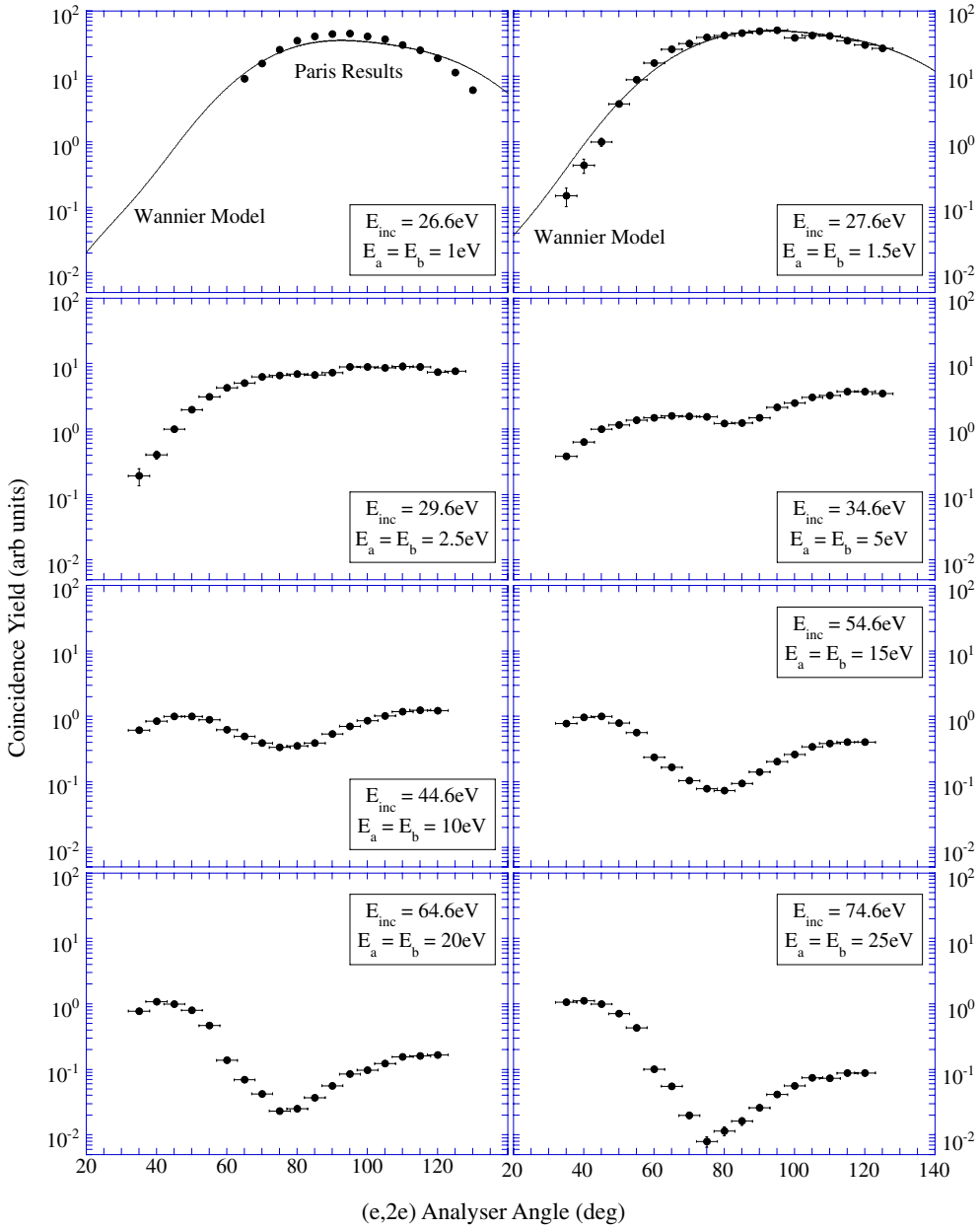

Figure 5. Differential cross-sections for the ionization of helium over a range of incident energies in a coplanar symmetric geometry reproduced here to allow comparison with figure 4. The data have been normalized to unity at $\xi = 45°$. The analysers are constrained between $\xi = 35°$ and 120° by the electron gun and Faraday cup. At the lower energies, calculations from the Wannier model are also shown, allowing the experimental results of [66] to be renormalized to unity at $\xi = 45°$. For details, see text.

depends on the valence electrons is not accurate. Comparison with previous results taken for helium show a marked contrast, even though the valence shells are similar. Electron correlations

are thought to be dominating the reaction over all energies that have been studied, in contrast to ionization from helium where post-collisional interactions play an increasingly important role as the energy decreases. These new results therefore provide a significant impetus for further theoretical exploration, as the dynamics of electron correlations are extremely difficult to model accurately.

Additional data which will help with this understanding are provided by superelastic scattering studies also carried out in this spectrometer [64]. These superelastic results have been successfully modelled at incident energies of 25 and 35 eV using a DWBA theory [70], and it remains to be seen whether this model can also predict the ionization cross-sections at these energies. The DWBA model of [70] fails to predict superelastic results accurately at an energy of 20 eV; however, models such as the CCC theory should be more accurate in this regime. The data on calcium presented in both of these studies cover a wide range of energy regimes where different models have been successful, and it is hoped that these results will help promote unification of these different theoretical approaches.

Acknowledgments

The Engineering and Physical Science Research Council is gratefully acknowledged for providing the funds to carry out this research. We would also like to thank Alan Venables, Dave Coleman and the members of the mechanical workshop at Manchester for providing excellent technical support for this research programme.

References

[1] Brunt J N H, King G C and Read F H 1976 *J. Phys. B: At. Mol. Phys.* **9** 2195
[2] Harting E and Read F H 1976 *Electrostatic Lenses* (Amsterdam: Elsevier)
[3] Comer J and Read F H 1971 *J. Phys. B: At. Mol. Phys.* **4** 368
[4] Weigold E and McCarthy I E 1978 *Adv. At. Mol. Phys.* **14** 127
[5] Lahmam-Bennani A 2002 *J. Electron Spectrosc.* **123** 365
[6] Duguet A, Cherid M, Lahmam-Bennani A, Franz A and Klar H 1987 *J. Phys. B: At. Mol. Phys.* **20** 6145
[7] Byron F W and Joachain C J 1989 *Phys. Rep.* **179** 211
[8] Zhang X, Whelan C T and Walters H R J 1990 *J. Phys. B: At. Mol. Opt. Phys.* **23** L509
[9] Rioual S, Pochat A, Gelebart F, Allan R J, Whelan C T and Walters H R J 1995 *J. Phys. B: At. Mol. Opt. Phys.* **28** 5317
[10] Rosel T, Roder J, Frost L, Jung K, Ehrhardt H, Jones S and Madison D H 1992 *Phys. Rev.* A **46** 2539
[11] Reid R H G, Bartschat K and Raeker A 1998 *J. Phys. B: At. Mol. Opt. Phys.* **31** 563
[12] Berakdar J, Klar H, Brauner M and Briggs J S 1990 *Z. Phys.* D **16** 91
[13] Wannier G H 1953 *Phys. Rev.* **90** 817
[14] Peterkop R 1971 *J. Phys. B: At. Mol. Phys.* **4** 513
[15] Rau A R P 1971 *Phys. Rev.* A **4** 207
[16] Bray I, Fursa D V, Kheifets A S and Stelbovics A T 2002 *J. Phys. B: At. Mol. Opt. Phys.* **35** R117
[17] Murray A J and Read F H 1992 *Phys. Rev. Lett.* **69** 2912
[18] Murray A J and Read F H 1993 *Phys. Rev.* A **47** 3724
[19] Murray A J, Woolf M B J and Read F H 1992 *J. Phys. B: At. Mol. Opt. Phys.* **25** 3021
[20] Murray A J and Read F H 1993 *J. Phys. B: At. Mol. Opt. Phys.* **26** L359
[21] Bowring N J, Read F H and Murray A J 1999 *J. Physique* **9** Pr6
[22] Bizau J M, Gerard P, Wuilleumier F J and Wendin G 1987 *Phys. Rev.* A **36** 1220
[23] Sato Y, Hayaishi T, Itikawa Y, Itoh Y, Murakami J, Nagata T, Sasaki T, Sonntag B, Yagashita A and Yoshino M 1985 *J. Phys. B: At. Mol. Phys.* **18** 225
[24] Ueda K, West J B, Ross K J, Hamdy H, Beyer H J and Kleinpoppen H 1993 *Phys. Rev.* A **48** R863
[25] West J B, Ueda K, Kabachnik N M, Ross K J, Beyer H J and Kleinpoppen H 1996 *Phys. Rev.* A **53** R9
[26] Ueda K, West J B, Ross K J, Kabachnik N M, Beyer H J, Hamdy H and Kleinpoppen H 1997 *J. Phys. B: At. Mol. Opt. Phys.* **30** 2093

[27] Beyer H J, West J B, Ross K J and De Fanis A 2000 *J. Phys. B: At. Mol. Opt. Phys.* **33** L767
[28] Mansfield M W D and Newsom G H 1977 *Proc. R. Soc.* **357** 77
[29] Ueda K, Kabachnik N M, West J B, Ross K J, Beyer H J, Hamdy H and Kleinpoppen H 1998 *J. Phys. B: At. Mol. Opt. Phys.* **31** 4331
[30] Fiquet-Fayard F and Lahmani M 1962 *J. Chem. Phys.* **59** 1050
[31] Okudaira S 1970 *J. Phys. Soc. Japan* **29** 409
[32] McFarland R H 1967 *Phys. Rev.* **159** 20
[33] Okuno Y 1971 *J. Phys. Soc. Japan* **31** 1189
[34] Vainstein L A, Ochkur V I, Rakhovskii V I and Stepanov A M 1972 *Sov. Phys.—JETP* **34** 271
[35] Cvejanovic D and Murray A J 2003 *J. Phys. B: At. Mol. Opt. Phys.* **36** 3591
[36] Schmitz W, Breuckmann B and Mehlhorn W 1976 *J. Phys. B: At. Mol. Phys.* **9** L493
[37] Pejcev V, Ottley T W, Rassi D and Ross K J 1978 *J. Phys. B: At. Mol. Phys.* **11** 531
[38] Feuerstein B, Zatsarinny O I and Mehlhorn W 2000 *J. Phys. B: At. Mol. Opt. Phys.* **33** 1237
[39] Weber W, Breuckmann B, Huster R, Menzel W, Mehlhorn W, Chen M H and Dyall K G 1988 *J. Electron Spectrosc.* **47** 105
[40] Chen M H, Weber W and Mehlhorn W 1989 *J. Electron Spectrosc.* **49** 77
[41] Hamdy H, Beyer H J and Kleinpoppen H 1990 *J. Phys. B: At. Mol. Opt. Phys.* **23** 1671
[42] Stevenson M, Dogan M and Crowe A 2003 *Int. Symp. on (e,2e), Double Photoionisation and Related Topics (Frankfurt, 2003)* abstract 8
[43] Weigold E 1991 *Aust. J. Phys.* **44** 277
[44] Elliott A, Lower J, Weigold E, Berakdar J, Engelns A and Klar H 1998 *Phys. Rev. Lett.* **80** 257
[45] Dorn A, Elliott A, Lower J and Weigold E 1998 *J. Electron Spectrosc.* **88** 59
[46] Weigold E, Berakdar J and Mazevet S 2001 *Phys. Rev. Lett.* **86** 624
[47] Frost L and Weigold E 1982 *J. Phys. B: At. Mol. Phys.* **15** 2531
[48] Streun M, Baum G, Blask W, Rasch J, Bray I, Fursa D V, Jones S, Madison D H, Walters H R J and Whelan C T 1998 *J. Phys. B: At. Mol. Opt. Phys.* **31** 4401
[49] Haynes M A and Lohmann B 2003 *XXIII ICPEAC* abstract We077 (unpublished)
[50] van Boeyen R W, Doering J P, Moore J H, Coplan M A and Cooper J W 2002 *J. Phys. B: At. Mol. Opt. Phys.* **35** L97
[51] Martin N L S, Bauman R P, Thompson D B, Wilson M and Ross K J 1996 *J. Phys. B: At. Mol. Opt. Phys.* **29** 4457
[52] Martin N L S, Bauman R P and Wilson M 1999 *Phys. Rev.* A **59** 2764
[53] Martin N L S, Bauman R P and Wilson M 1998 *Phys. Rev.* A **57** 1827
[54] Martin N L S and Thompson D B 1991 *Phys. Rev.* A **43** 2281
[55] Martin N L S, Bauman R P and Wilson M 1998 *Phys. Rev.* A **57** 4346
[56] Kull T, Nakel W and Schroter C D 1997 *J. Phys. B: At. Mol. Opt. Phys.* **30** L815
[57] Walters H R J, Ast H, Whelan C T, Dreizler R M, Graf H, Schroter C D, Bonfert J and Nakel W 1992 *Z. Phys.* D **23** 353
[58] Murray A J, Turton B C H and Read F H 1992 *Rev. Sci. Instrum.* **63** 3346
[59] Cvejanovic D and Murray A J 2002 *Meas. Sci. Technol.* **13** 1482
[60] Murray A J 2002 *Meas. Sci. Technol.* **13** N12
[61] Murray A J and Atkinson S 2003 *Meas. Sci. Technol.* submitted
[62] Brunt J N H, King G C and Read F H 1977 *J. Phys. B: At. Mol. Phys.* **10** 1289
[63] Murray A J 2001 *Photonic Electronic and Atomic Collisions* (Princeton, NJ: Rinton Press) p 437
[64] Murray A J and Cvejanovic D 2003 *J. Phys. B: At. Mol. Opt. Phys.* **36** 4889
[65] Murray A J and Cvejanovic D 2003 *XXIII ICPEAC* abstract Mo74
[66] Selles P, Huetz A and Mazeau J 1987 *J. Phys. B: At. Mol. Phys.* **20** 5195
[67] Murray A J, Read F H and Bowring N J 1994 *Phys. Rev.* A **49** R3162
[68] Hawley-Jones T J, Read F H, Cvejanovic S, Hammond P and King G 1992 *J. Phys. B: At. Mol. Opt. Phys.* **25** 2393
[69] Walters H R J, Zhang X and Whelan C T 1993 (*e*, 2*e*) *and Related Processes* (Dordrecht: Kluwer) p 33
[70] Srivastava R, Zuo T, McEachran R P and Stauffer A D 1992 *J. Phys. B: At. Mol. Opt. Phys.* **25** 3709